Resolving the Rise and Fall of Star Formation in Galaxies
Proceedings IAU Symposium No. 373, 2023
T. Wong & W.-T. Kim, eds.
doi:10.1017/S1743921322003994

Radiatively Cooling Superwinds in Ultracompact H II Regions

A. Danehkar

Eureka Scientific, 2452 Delmer Street, Suite 100, Oakland, CA 94602-3017, USA
email: danehkar@eurekasci.com

Abstract. Ultracompact H II regions (UC-HII) are the young, very dense cores of massive star-forming regions in dwarf galaxies, where newly formed massive OB stars are surrounded by natal molecular clouds. Thermal energy deposited by mechanical feedback from a cluster of massive OB stars can form a superwind, which may lead to a wind-blown bubble as well as radiative cooling. We investigate the formation of radiatively cooling superwinds in UC-HII using a radiative cooling module in the hydrodynamics program FLASH. We built a grid of hydrodynamic simulations to determine the dependence of radiative cooling on the cluster radius, mass-deposition rate, wind velocity, and ambient medium in UC-HII. Our findings could help to better understand star formation in massive star-forming regions, where cool superwinds could trigger the formation of molecular clumpy regions.

Keywords. Stars: winds – ISM: bubbles – radiation mechanisms – galaxies: starburst

---

The deposition of energy and momentum by young, massive OB stars into the interstellar medium (ISM) produces superwinds on parsecs to kpc scales (Heckman et al. 1990; Lehnert & Heckman 1995; Veilleux et al. 2005), whose cooling outflow feedback can promote star formation in giant molecular clouds (Fabian et al. 1984; Krause et al. 2016). The shock-ionization by superwinds often generates X-ray bubbles (Strickland et al. 1997; Martin 1999; Ott et al. 2005). Contemporary surveys of some compact star-forming regions such as those in NGC 5253 (Turner et al. 2017) and Mrk 71 (Oey et al. 2017) suggested the presence of excessive cooling effects beyond the adiabatic predictions. This is generally attributed to radiatively cooling superwinds, as shown by semi-analytical numerical results (Silich et al. 2004; Tenorio-Tagle et al. 2005) and adaptive mesh hydrodynamic simulations (Gray et al. 2019a; Danehkar et al. 2021).

One of the earliest stages in the evolution of an H II region is the so-called ultracompact H II (UC-HII) region (Wood & Churchwell 1989), which is very dense ($\gtrsim 10^4$ cm^{-3}) surrounding a compact (< 0.1 pc) stellar cluster having a lifetime of $\lesssim 0.1$ Myr (see the review by Churchwell 2002). In such compact regions, the youngest OB stars are present, which ionize the surrounding ISM and produce superwinds on a small scale ($\lesssim 10$ pc) (Hoare et al. 2007; Olivier et al. 2021), leading to hot, wind-blown bubbles (see e.g. Tsujimoto et al. 2006) and shells (De Pree et al. 2000). The cool gas formed by a superwind in UC-HII could also stimulate the formation of new stars in giant molecular clouds.

To learn more about radiatively cooling superwinds in UC-HII, we used the atomic chemistry and radiative cooling module MAIHEM (Gray et al. 2019b) in the hydrodynamics program FLASH (Fryxell et al. 2000) to run a set of hydrodynamic simulations of a spherical stellar wind model. We consider a stellar wind driven by thermal feedback from a stellar cluster described by the cluster radius $R_{\rm sc}$ being smaller than 1 pc in typical

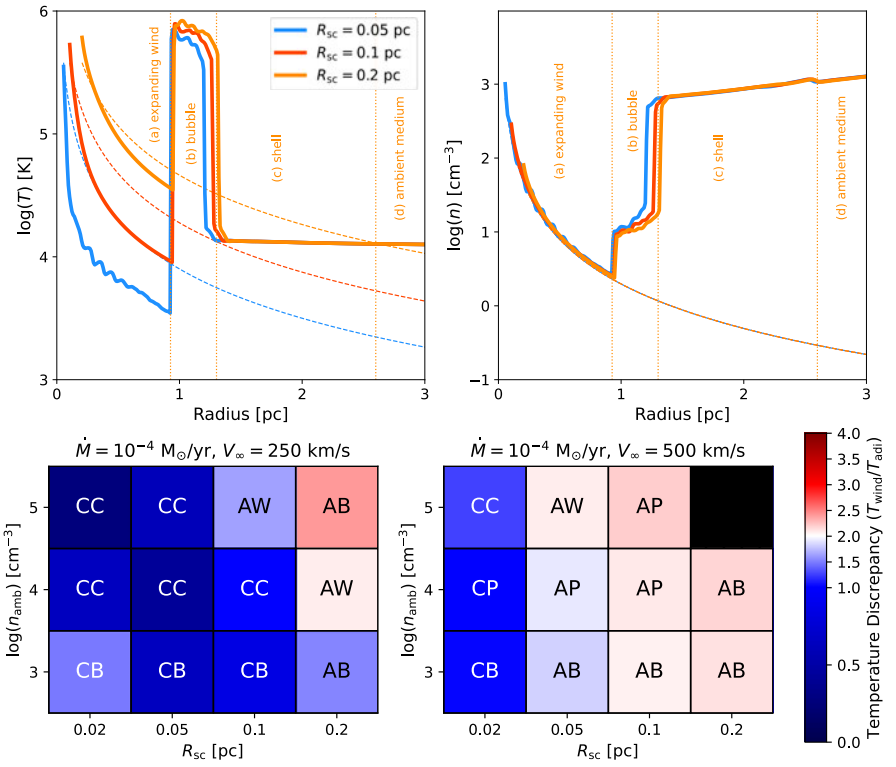

Figure 1. *Top Panels*: The temperature (T) and density (n) profiles (solid lines) along with the adiabatic predictions (dashed lines) for the models with $V_\infty = 250\,\mathrm{km\,s^{-1}}$, $\dot{M} = 10^{-4}\,\mathrm{M_\odot\,yr^{-1}}$, $t = 1\,\mathrm{Myr}$, $R_{sc} = 0.05$, 0.1, and 0.2 pc, $M_\star = 2\times10^4\,\mathrm{M_\odot}$, $n_{amb} = 10^3\,\mathrm{cm^{-3}}$, $Z/Z_\odot = 0.5$, and $t =$ 0.1 Myr. The expanding wind region, bubble, shell, and the ambient medium for $R_{sc} = 0.2$ pc are separated by dotted lines. *Bottom Panel*: The average wind temperatures T_{wind} produced by our hydrodynamic simulations with respect to the average adiabatic predictions T_{adi} for the wind velocities $V_\infty(t) = 250$ and 500 $\mathrm{km\,s^{-1}}$, mass-deposition rate $\dot{M}(t) = 10^{-4}\,\mathrm{M_\odot\,yr^{-1}}$, metallicity $Z/\mathrm{Z_\odot} = 0.5$, ambient densities $\log n_{amb} = 3$, 4, and $5\,\mathrm{cm^{-3}}$, and stellar radii $R_{sc} = 0.02$, 0.05, 01, and 0.2 pc, total stellar mass $M_\star = 2\times10^4\,\mathrm{M_\odot}$, and age $t = 0.1$ Myr. The wind modes (AW, AB, AP, CC, CB, and NW) are classified according to the criteria by Danehkar et al. (2021).

H II regions, mass-deposition rate $\dot{M}$, wind velocity V_∞, and the radiation field made by Starburst99 (Leitherer et al. 1999) for a total stellar mass of $M_\star = 2\times10^4\,\mathrm{M_\odot}$, and ambient density n_{amb} higher than typical evolved H II regions considered in Danehkar et al. (2021). Figure 1 shows the temperature and density profiles (top panels) of three wind models simulated by MAIHEM for different cluster radii $R_{sc} = 0.05$, 01, and 0.2 pc. For comparison, the adiabatic temperature and density profiles were also plotted using dashed lines. Each model has four regions (as defined by Weaver et al. 1977), namely expanding wind, hot bubble, shell, and ambient medium, shown for $R_{sc} = 0.2$ pc in Fig. 1. With fixed wind parameters, it can be seen that models with smaller cluster radii have stronger radiative cooling.

Figure 1 presents various wind modes (bottom panel) for UC-HII regions with dense ambient densities ($n_{amb} = 10^3$, 10^4, and $10^5\,\mathrm{cm^{-3}}$), compact cluster radii ($R_{sc} = 0.02$, 0.05, 01, 0.2 pc), produced for tow different wind velocities $V_\infty = 250$ and 500 $\mathrm{km\,s^{-1}}$ and mass-deposition rate $\dot{M}(t) = 10^{-4}\,\mathrm{M_\odot\,yr^{-1}}$. We employ the superwind classification by Danehkar et al. (2021) according to energy- or momentum-conserving, the presence or absence of a bubble, and an adiabatically or radiatively cooled thermal curve. The

https://doi.org/10.1017/S1743921322003994 Published online by Cambridge University Press

adiabatic (AW) and catastrophic cooling (CC) modes are those without any wind-blown bubble, whereas adiabatic bubble (AB) and catastrophic cooling bubble (CB) modes have a thermal bubble. Moreover, the adiabatic, pressure-confined (AP) mode has a hot bubble being stalled by the surroundings thermal pressure. The no wind (NW) mode is assigned to a superwind suppressed by a high ambient pressure. It can be seen that reducing the cluster radii increases radiative cooling in superwinds. Moreover, we again spot the dependency of cooling on the wind velocity and mass-deposition rate similar to what Danehkar et al. (2021) obtained for more evolved H II regions with ambient densities less than $10^3\,\mathrm{cm}^{-3}$ and the typical cluster radius of 1 pc.

Recently, Danehkar et al. (2021, 2022) utilized the radial profiles of the density, temperature, and non-equilibrium ionization (NEI) states made by MAIHEM for evolved H II regions to produce the line emissivities using the photoionization program CLOUDY (Ferland et al. 2017) for combined collisional ionization and photoionization, as well as non-equilibrium photoionization conditions. Danehkar et al. (2022) found that in metal-poor regions, the O VI lines were stronger when photoionization is not in equilibrium. O VI lines were previously proposed for tracing radiative cooling in H II regions (Gray et al. 2019a,b). In particular, the nearest Lyman-break analog, Haro 11, was found to emit O VI, which could originate from radiative cooling (Grimes et al. 2007). Further numerical modeling of superwinds driven by stellar clusters with the physical properties seen in UC-HII will be great for identifying compact coolants formed by radiatively cooling in massive star-forming regions.

References

Churchwell E., 2002, ARA&A, 40, 27
Danehkar A., Oey M. S., Gray W. J., 2021, ApJ, 921, 91
Danehkar A., Oey M. S., Gray W. J., 2022, ApJ, 937, 68
De Pree C. G., Wilner D. J., Goss W. M., Welch W. J., McGrath E., 2000, ApJ, 540, 308
Fabian A. C., Nulsen P. E. J., Canizares C. R., 1984, Nature, 310, 733
Ferland G. J. et al., 2017, RMxAA, 53, 385
Fryxell B. et al., 2000, ApJS, 131, 273
Gray W. J., Oey M. S., Silich S., Scannapieco E., 2019a, ApJ, 887, 161
Gray W. J., Scannapieco E., Lehnert M. D., 2019b, ApJ, 875, 110
Grimes J. P. et al., 2007, ApJ, 668, 891
Heckman T. M., Armus L., Miley G. K., 1990, ApJS, 74, 833
Hoare M. G., Kurtz S. E., Lizano S., Keto E., Hofner P., 2007, in Protostars and Planets V, Reipurth B., Jewitt D., Keil K., eds., Tucson: University of Arizona Press, p. 181
Krause M. G. H., Charbonnel C., Bastian N., Diehl R., 2016, A&A, 587, A53
Lehnert M. D., Heckman T. M., 1995, ApJS, 97, 89
Leitherer C. et al., 1999, ApJS, 123, 3
Martin C. L., 1999, ApJ, 513, 156
Oey M. S., Herrera C. N., Silich S., Reiter M., James B. L., et al., 2017, ApJ, 849, L1
Olivier G. M., Lopez L. A., Rosen A. L., Nayak O., Reiter M., et al., 2021, ApJ, 908, 68
Ott J., Walter F., Brinks E., 2005, MNRAS, 358, 1453
Silich S., Tenorio-Tagle G., Rodríguez-González A., 2004, ApJ, 610, 226
Strickland D. K., Ponman T. J., Stevens I. R., 1997, A&A, 320, 378
Tenorio-Tagle G., Silich S., Rodríguez-González A., Muñoz-Tuñón C., 2005, ApJ, 620, 217
Tsujimoto M., Hosokawa T., Feigelson E. D., Getman K. V., Broos P. S., 2006, ApJ, 653, 409
Turner J. L., Consiglio S. M., Beck S. C., Goss W. M., et al., 2017, ApJ, 846, 73
Veilleux S., Cecil G., Bland-Hawthorn J., 2005, ARA&A, 43, 769
Weaver R., McCray R., Castor J., Shapiro P., Moore R., 1977, ApJ, 218, 377
Wood D. O. S., Churchwell E., 1989, ApJ, 340, 265

https://doi.org/10.1017/S1743921322003994 Published online by Cambridge University Press